Carbohydrate Polymers 114 (2014) 253–259

Contents lists available at ScienceDirect

Carbohydrate Polymers

journal homepage: www.elsevier.com/locate/carbpol

Synthesis and application of polypyrrole/carrageenan nano-bio composite as a cathode catalyst in microbial fuel cells

Chakavak Esmaeili[a], Mostafa Ghasemi[b,c,*], Lee Yook Heng[a], Sedky H.A. Hassan[d,e], Mahnaz M. Abdi[f], Wan Ramli Wan Daud[b,c], Hamid Ilbeygi[g], Ahmad Fauzi Ismail[h]

[a] School of Chemical Sciences and Food Technology, Faculty of Science and Technology, Universiti Kebangsaan Malaysia—UKM, 43600 Bangi, Selangor, Malaysia
[b] Fuel Cell Institute, Universiti Kebangsaan Malaysia—UKM, 43600 Bangi, Selangor, Malaysia
[c] Department of Chemical and Process Engineering, Faculty of Engineering and Built Environment, Universiti Kebangsaan Malaysia—UKM, 43600 Bangi, Selangor, Malaysia
[d] Botany Department, Faculty of Science, Assiut University, New Valley Branch, New Valley, Egypt
[e] Department of Biological Environment, Kangwon National University, 200-701 Chuncheon, Kangwon-do, South Korea
[f] Department of Chemistry, Faculty of Sciences, Universiti Putra Malaysia, 43400 Serdang, Selangor D.E., Malaysia
[g] Australian Institute for Bioengineering and Nanotechnology (AIBN), University of Queensland, Brisbane 4072, QLD, Australia
[h] Advanced Membrane Technology Research Centre (AMTEC), Universiti Teknologi Malaysia, 81310 Johor Bahru, Johor, Malaysia

ARTICLE INFO

Article history:
Received 28 March 2014
Received in revised form 7 July 2014
Accepted 29 July 2014
Available online 13 August 2014

Keywords:
Kappa-carrageenan
Polypyrrole
Nano-bio composite
Cathode catalyst
Microbial fuel cell

ABSTRACT

A novel nano-bio composite polypyrrole (PPy)/kappa-carrageenan(KC) was fabricated and characterized for application as a cathode catalyst in a microbial fuel cell (MFC). High resolution SEM and TEM verified the bud-like shape and uniform distribution of the PPy in the KC matrix. X-ray diffraction (XRD) has approved the amorphous structure of the PPy/KC as well. The PPy/KC nano-bio composites were then studied as an electrode material, due to their oxygen reduction reaction (ORR) ability as the cathode catalyst in the MFC and the results were compared with platinum (Pt) as the most common cathode catalyst. The produced power density of the PPy/KC was 72.1 mW/m^2 while it was 46.8 mW/m^2 and 28.8 mW/m^2 for KC and PPy individually. The efficiency of the PPy/KC electrode system is slightly lower than a Pt electrode (79.9 mW/m^2) but due to the high cost of Pt electrodes, the PPy/KC electrode system has potential to be an alternative electrode system for MFCs.

1. Introduction

The increasing demand for fossil fuels coupled with global warming associated with certain environmental concerns has caused a global movement towards the generation of renewable energy. As such, wastewater can be considered a valuable source for the generation of renewable energy in the form of biodegradable organic matters (Ghasemi et al., 2013a). As wastewater treatment plants have high capital costs, energy extraction from wastewater is valuable in the production of renewable energy. Microbial fuel cell (MFC) is a device that generates electricity from organic compounds by using microorganisms as a biocatalyst. It means that a MFC is a device that simultaneously generates electricity while treating wastewater. The advantages of the MFC compared to current technologies such as membrane treatment or anaerobic digestion is its lower costs and potentially high energy efficiency as electricity would be produced directly without any inefficient steps or wastage of materials. A number of factors affect the performance of the MFC such as the microbial inoculums, the proton exchange membrane, internal and external cell resistance, the cathode catalyst and the electrode spacing. Among these factors, the cathode catalyst attracts more attention from researchers. Pt as the common cathode catalyst covers about 50% of the total MFC cost.

Nowadays, intrinsically conducting polymers have attracted a lot of attention in the area of advanced materials, such as polyaniline (PANI), sulfonated PANI (SPAN)-Fe_3O_4 nanocomposites (Reddy, Lee, & Iyengar, 2007), PANi functionalized multi-walled carbon nanotubes with metal nanoparticles (Reddy et al., 2009). Among conducting polymers PPy and its composite exhibit highly attractive for variety of their application because of it is environmentally stable, easy to synthesize and highly conductive as

* Corresponding author at: Fuel Cell Institute, Universiti Kebangsaan Malaysia—UKM, 43600 Bangi, Selangor, Malaysia. Tel.: +60 3 8911 8588; fax: +60 3 89215064.
E-mail addresses: mostafag@eng.ukm.my, mostafghasemi@gmail.com (M. Ghasemi).

http://dx.doi.org/10.1016/j.carbpol.2014.07.072
0144-8617/

well as showing a low electropolymerization of PPy compared to other conductive polymer which allows PPy and its composite stay stable under ambient conditions (Ates, Karazehir, & Sarac, 2012). PPy can be used in biosensors, wires, catalysts and anti-electrostatic coatings (Apetrei & Apetrei, 2013; Safarnavadeh, Zare, & Fakhari, 2013). PPy revealed its biocompatibility through strong interactions with other polymers (Colin & Petit, 2002), and bio molecules (Arora et al., 2006). Thus, polymer composites based on polyconjugated systems create large surface membranes due to the enhancement of conductivity and sensitivity that create stronger catalytic activity. The stabilizing of composites is essential for a variety of applications such as bio (sensor) (Lupu et al., 2013), fuel cell (Ghasemi et al., 2013d), photovoltaic cell (Zhang et al., 2013) and catalysis (Liu et al., 2013). Composite polymers can be synthesized using chemical, electrochemical polymerization and self-assembly process (Reddy, Jeong, Lee, & Raghu, 2010; Reddy, Lee, & Gopalan, 2007). The preparation of well-known composite polymers as catalysts facilitates the modification of a conducting PPy. PPy inorganic composites have been previously used as the cathode or anode electrode in an MFC but in this study PPy, as an inorganic conducting polymer and kappa-carrageenan (KC) biopolymer have been used as the novel nano-bio composite catalyst in a MFC. The composite formations from intrinsically conducting polymers are much different than inorganic conducting polymers. In the other word, composite formation, in conducting polymers is interstitial whereas the composite formation in inorganic conducting polymer is substitution and also, making composite in the conducting polymer is reversible in a way, unlike inorganic polymer, on the other hand, the original polymer can be maintained with no degradation of the polymer backbone (Bakhshi & Bhalla, 2004). The chemical polymerization method has been used due to couple of advantages when compared with the electrochemical method. First, the chemical method is unlimited in terms of the production and collection of composites and second, the chemical method is suitable for the preparation of composite thin films with controlled thickness above 100 nm or of nano size. The composite polymer of KC is not only biodegradable, but is also edible (Alves et al., 2011). KC is known as an acidic hydrophilic polyanion and is also used in the food industry as a gelling and thickening reagent. This polyanion with OSO_3^- (sulphate) functional group makes an intramolecular bridge into the positive charge of the PPy due to the growth of the composites (Colin & Petit, 2002). In addition, KC possesses water retention abilities due to hydrogen bonding and it exhibits high proton conductivity (Fujishima et al., 2008) and KC has not been studied for fuel cell application in till now and in this field seems to be very novel and efficient. The chemical polymerization process is suitable for the synthesizing of PPy/KC composites with controlled thickness and is unlimited in terms of the collection and production of composites.

The electrochemical method has two disadvantages compared to traditional chemical polymerization. One is that the electrochemical method is limited in terms of the mass production of composite electrodes and the other is that the electrochemical method is not suitable for preparing controlled polymer films with thicknesses above 100 mm. However it is proper for preparing very thin films of polymer (Martínez-Huitle & Brillas, 2009).

This method shows that PPy/KC produces as much power and is a simple method utilizing cheaper chemicals than Pt.

The modification of composite polymers by making nanocomposite has attracted a lot of attention due to (Dharuman, Hahn, Jayakumar, & Teng, 2013), improvement of catalytic activity (Nguyet et al., 2013) and production of larger surface area substances.

So for the first time, the nano-bio composite has been used as an alternative for Pt in MFCs to see the effect of that in the MFCs. The results have been compared with Pt as the common cathode catalyst, PPy as the source of polymer and KC as the biopolymer in this paper.

2. Experimental

2.1. Materials

The pyrrole monomer was obtained from Acros Organics. Kappa-carrageenan was purchased from Fluka. Iron(III) chloride ($FeCl_3$) was provided by Sigma Aldrich. The phosphate buffer solution was prepared using K_2HPO_4 and KH_2PO_4 purchased from Merck. Deionised water is used during the experiment.

2.2. Synthesis of PPy and kappa-carrageenan composite

Various amounts of kappa-carrageenan (KC) powder were dissolved in deionised water. KC bio-polymer dissolve in 40 ml of deionized water and then was mixed with the 0.684 g of pyrrole (pre-distilled) by stirring at 40 °C for 10 min continuously. An aqueous solution of the oxidant 10 ml of ($FeCl_3$) in distilled water was added up drop-wise to the mixture. The total volume of the deionized water was used 50 ml. The molar ratio of the $FeCl_3$/pyrrole was always kept at 2:3 (Brezoi, 2010). Formation of black PPy precipitate was clearly observed immediately after the addition of the oxidant. The polymerization process was carried out for 45 min at room temperature by moderate stirring. After optimum condition of KC has been achieved, the KC and PPy were mixed together in 1.46:98.54 wt%.

First, the black precipitate was filtered off, then has been washed it with distilled water, and centrifuged several times in order to isolate the sample. The black kappa-carrageenan–polypyrrole (PPy/KC) powder was then dried in the oven at 60 °C for 5 h. It should be noted that, the electrical properties of the composite are governed by the amount of KC concentration and the results demonstrated that KC properties are affected by changing the temperature employed during concentration of KC solution as well as the KC of dispersant into composite formed.

2.3. MFC configuration

Two cubic shaped chambers were constructed from Plexiglas, with a height of 10 cm, width of 6 cm and length of 10 cm (giving a working volume of 420 ml). They were separated by a Nafion 117 Proton Exchange Membrane (PEM). Oxygen was continuously fed into the cathode by an air pump at a rate of 80 ml/min. Both the cathode and the anode projected surface areas of 12 cm^2. The cathode was carbon paper, coated with 0.5 mg/cm^2 Pt and the anode (as described above) was plain carbon paper (Ghasemi et al., 2011; Rahimnejad et al., 2012).

2.4. Enrichment

Palm Oil Mill Effluent (POME, Indah Water Konsortium) anaerobic sludge was used for the inoculation of the MFCs. The media contained 5 g of glucose, 0.07 g of yeast extract, 0.2 g of KCl, 1 g of $NaH_2PO_4{\cdot}4H_2O$, 2 g of NH_4Cl, 3.5 g of $NaHCO_3$ (all from the Merck company), 10 ml of Wolfe's mineral solution and 10 ml of Wolfe's vitamin solution (added per litre). All experiments were conducted in an incubator at 30 °C. Furthermore, the cathode chamber contained a phosphate buffer solution, which consisted of 2.76 g/l of NaH_2PO_4, 4.26 g/l of Na_2HPO_4, 0.31 g/l of NH_4Cl and 0.13 g/l of KCl (all from the Merck company) (Rahimnejad et al., 2012).

2.5. Analysis and calculation

The sizes and the surface morphology of KC, PPy and PPy/KC composites were investigated by the using a scanning electron microscope (LEO 1450VP, Germany) at an accelerated voltage of 3.00 kV. SEM–energy-dispersive X-ray (EDX) spectroscopy enables the measurement of chemical compositions, such as carbon, oxygen and nitrogen, of the polymers and composite (VPSEM-EDX; Philips XL 30, Eindhoven, Netherlands). Nicolet 5700 FTIR (Thermo Electron, USA) was performed to identify the functional group of the samples. Also, VPSEM was used for observing the attachment of microorganisms on the anode electrode. Transmission electron microscopy (TEM, Philips CM12) was employed to study the size and flake thickness of the composite particles. The average size and the standard deviation of the composite particles were calculated from at least 50 particles of the composites. To study the structure of the materials and composites, the X-ray diffraction (XRD) technique was used by utilizing a Siemens D5000 advance diffractometer using a monochromatic Cu$K\alpha$ as the radiation source ($\lambda = 1.5418$ Å) at a scanning rate of $0.02^\circ\ s^{-1}$ for 2θ range from 20° and 80°.

To measure the chemical oxygen demand (COD), samples were first diluted 10 times and 2 ml of the diluted samples were mixed with a digestion solution of a high-range COD reagent, then heated at 150 °C for 2 h in a thermoreactor (DRB200), which was read with a spectrophotometer (DR 2800). The voltage was measured using a multimeter (Fluke 8846A) and the power density curve was obtained by applying different loads to the system and calculating the power at the different loads.

The current was measured using the:

$$I = \frac{V}{R} \tag{1}$$

where I is the current (amps), V is the voltage (volt) and R is the applied external resistance (ohm).

The power density was calculated using the following equation:

$$P = R \times I^2 \tag{2}$$

where R is the applied external resistance (ohm) and I is the current (amps) (calculated using Eq. (1).

The coulombic efficiency (CE) was calculated as the current over time, until the maximum theoretical current was achieved. The evaluated CE over time was calculated using the following equation:

$$\mathrm{CE} = \frac{M \int_0^t I\mathrm{d}t}{FbV_{\mathrm{an}}\Delta\mathrm{COD}} \tag{3}$$

where M is the molecular weight of oxygen (32), F is Faraday's constant, $b = 4$ indicates the number of electrons exchanged per mole of oxygen, V_{an} is the volume of liquid in the anode compartment and ΔCOD is the change in chemical oxygen demand (COD) over time, 't'.

2.6. Pre-treatment of Nafion 117

The PEM should be pre-treated before applying in the MFC. Nafion 117 first has to be boiled in distilled water for 1 h. Then it has to be soaked in 3% hydrogen peroxide and 0.5 M sulphuric acid, each one for 1 h. The pre-treated Nafion 117 should be stored in water before use (Ghasemi, Shahgaldi, Ismail, Yaakob, & Daud, 2012).

2.7. Cyclic voltammetry (CV) and liner sweep voltammetry (LSV)

The cyclic voltammetry (CV) experiment was carried out with a potentiostat Autolab PGSTAT 12 (Autolab, Metrohm) in the voltage range of −1.0 V to 1.0 V during five cycles with the scan rate of 50 mV/s. The LSV test has been done to measure the catalytic activity and to make a comparison of the liberated electrons 0.1 M H_2SO_4, using Ag/AgCl as the reference electrode with a 50 mV/S scan rate.

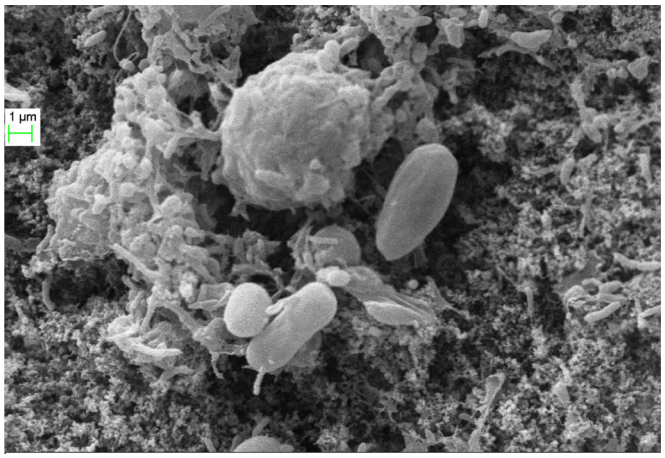

Fig. 1. Attachment of microorganisms on anode electrode.

3. Results and discussion

3.1. Attachment of microbial community on the anode surface

Fig. 1 shows the attachment of microorganisms on the surface of the anode electrode when the MFC is in stable condition. As can be seen in the figure, different types of microorganisms attached onto the electrode surface. These play the significant role of biocatalyst in the anode. The microorganisms produce protons and electrons by consumption of organic compounds of substrates in the anode chamber (Ghasemi et al., 2011).

3.2. XRD

The XRD patterns of the KC, PPy and PPy/KC composites are shown in Fig. 2a. In this work, PPy and KC were utilized as references. The pure KC illustrated a strong reflection to the Bragg angles (2θ) which usually reports signals at 28.5° (Chen, Peng, Lei, Liu, & Zhao, 2013).

Diffractograms of the PPy showed a broad scattering of peaks at approximately 9° and 25.8°, which indicate a highly amorphous structure that is similar to those reported for PPy (Abdi et al., 2010). The PPy/KC composite showed a different diffraction pattern compared to pure KC and PPy. The composite showed the homogeneous formation and amorphous structure of the PPy in the presence of the KC. The diffractograms of the PPy film and the PPy/KC composite film look alike with broad scattering maxima at 2θ values of 14.5° and 33.5° which indicate a highly amorphous structured composite and the homogeneous composite formation of polypyrrole with KC. PPy–KC composite is formed in such a manner that the structure is uniform over relatively homogenous distance, the lattice spacing in the composite being essentially constant from one grain to another for any particular with respect to the pressure of composite whilst, the pressure of PPy has not been seen.

Also the FTIR of the composite was shown in Fig. 2b.

Fig. 2b displays the FTIR spectra of pure KC, PPy and KC–PPy composite. In the present workup, the peak in Graph 2.b related to KC, at approximately 847 cm^{-1}, indicates D-galactose-4-sulfate of kappa-carrageenan spectra and the other peak at 1210–1260 cm^{-1} wasassigned to strong bands owing to the S=O band of sulphate

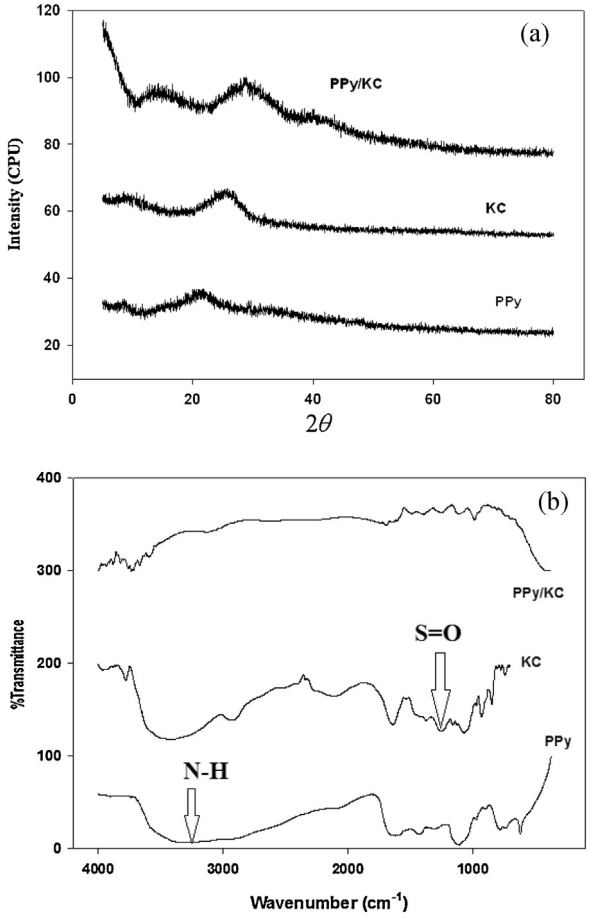

Fig. 2. (a) XRD patterns of PPy, KC and PPy/KC, (b) FTIR of PPy, KC and PPy/KC composite.

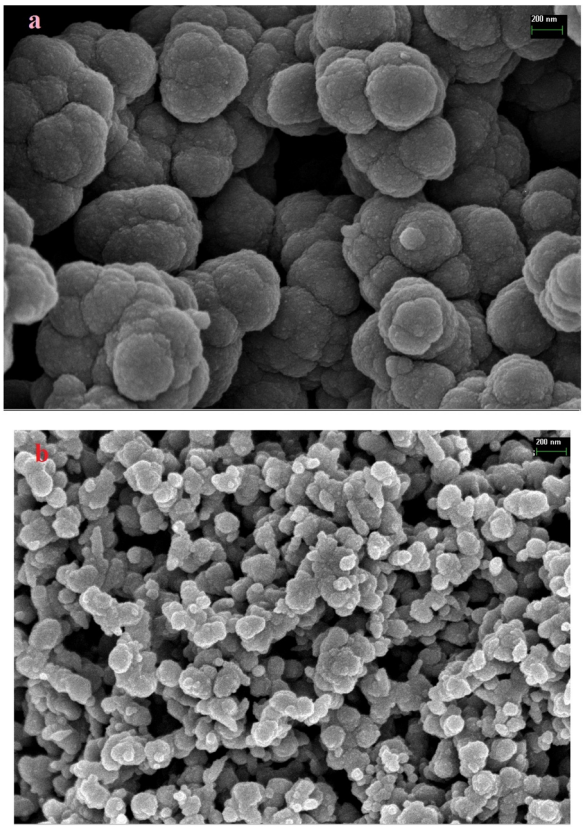

Fig. 3. SEM image of (a) PPy and (b) PPy/KC.

ester and the strong —OH group vibrations band at approximately 3436 cm^{-1}, in addition to the glycosidic linkage seen at 1010–1080 cm^{-1}. Graph 2.b depicts the FTIR functional group study of polypyrrole (PPy) ring. In this spectrum, the vibration band of C—H and C=C in the PPy were ascribed at 2950 cm^{-1} and 1420 cm^{-1}, respectively, and the sharp peak at 3450 cm^{-1} was related to the N—H stretching band.

Graph 2.b was also related to the functional group of nanocomposite, as confirmed using FTIR spectroscopy of PPy–KC composite conjugation. The composite was overlapped with the PPy and KC characteristic absorption peaks. The nucleophilic electron pair from PPy attacks the carbon of the carrageenan attached to sulphate (OSO_3^-); due to the formation of a new bond. Meanwhile, the sulphate (as a good leaving group) departs with an electron pair of the N—H absorption band of PPy the N—H deformation vibration at 3450 cm^{-1}, appears at the same position in the spectra of the KC–PPy composite.

As mentioned above, the absorption of the S=O band at 1210–1260 cm^{-1} region disappeared and the N—H band at 3450 cm^{-1} in the composite product was lower than in kappa-carrageenan and polypyrrole, respectively.

3.3. Scanning electron microscopy (SEM)

The surface morphology of the polymer and composite polymer were studied by SEM. Fig. 3, illustrates the SEM morphology from the fraction surface of the PPy (a) and the PPy/KC composite (b). It has already shown that KC has a porous structure via interconnection in a three-dimensional microstructure (Sadeghi, 2012). It is assumed that, homogenous microstructure and smoothly emulsified pure KC affect the behaviour of the droplets embedded in the KC hydrogel and also, the density of the PPy/KC composite dependence on the composite size, on the other hand, the size decrease by increasing density (Andrenacci, Pieri, & Strinati, 2000).

In Fig. 3a, the PPy displays a typically cauliflower-like spherical shape that is similar to those reported for PPy (Yalçınkaya, Demetgül, Timur, & Çolak, 2010). According to Fig. 4, the employment of ferric chloride as an oxidizing reagent causes the cauliflower formation and compact morphology (Shinde, Gund, Dubal, Jambure, & Lokhande, 2013). Further, the reaction between the free electron in the ferric chloride and one of the electrons of the pyrrole causes the breaking of the π bond in the pyrrole. Consequently, the formation of PPy happens by attacks of free electron in a pyrrole (as electron donating) to another pyrrole with π bond (as electron withdrawing) (Wang, Li, & Yang, 2001). The surface energy of KC/PPy composite polymer is higher than PPy, furthermore, able to strong interactions with electron donating and electron withdrawing forces (Saville, 2005) according to Fig. 3b the incorporation of PPy into KC the made composite bud-like structured with higher smoothness and homogenous dispersion properties which help to catalytic activity.

3.4. Transmission electron microscopy (TEM)

Fig. 5 shows the TEM images of the PPy/KC particles and their particle size distributions. The investigation of size distribution of the particles was performed by TEM analysis, counting at least 50 nanoparticles for a careful look at the picture to recognize the particle boundaries.

The software Image J (Roberts et al., 2007) was utilized to calculate the mean diameter of the core and the average thickness of shell on the surface of core. The obtained diameters were 106.79 nm

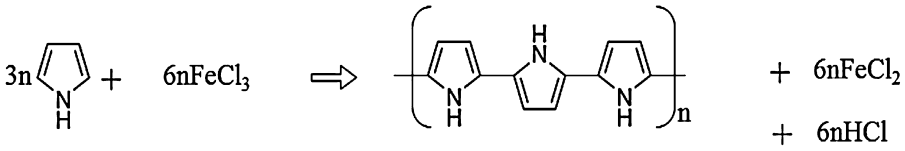

Fig. 4. The reaction mechanism of PPy polymerization by ferric chloride oxidizing agent [21].

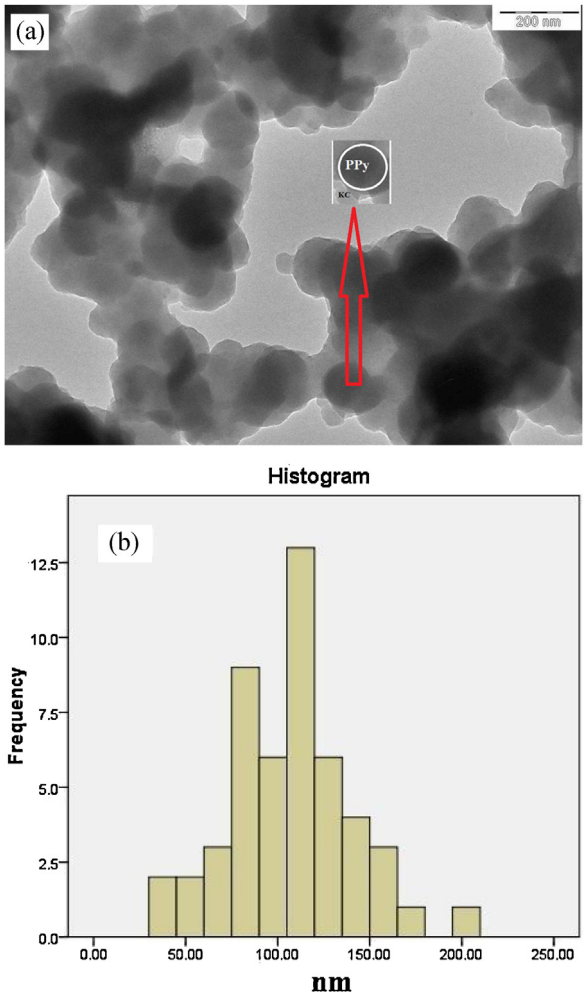

Fig. 5. (a) TEM image of PPy/KC composite, (b) histogram based on several TEM calculated via lognormal fitting.

and 142.3 nm, respectively, in addition, using a log–normal fitting of the histograms demonstrated in Fig. 5.

The PPy/KC particles demonstrated a nearly nano-size morphology which is attributed to the nano composite structure. The TEM morphology demonstrate that the size and homogenous of particles in composite that can be useful for catalytic application. Also as it has been shown in Fig. 5a the PPy particles have been covered by KC hydrogel as biopolymer. Fig. 5a exhibited that, the KC biopolymer due to the individual properties of outside nanocomposite layers will be formed as shell and PPy as core.

3.5. Cyclic voltammetry (CV)

Cyclic voltammograms were recorded using SPE modified with the PPy, KC and PPy/KC composites and are given in Fig. 6a. It can be observed that the KC had an effect on the redox properties of the resulting PPy/KC composite. The PPy/KC displayed improved redox characteristics when compared with those of the PPy and KC alone,

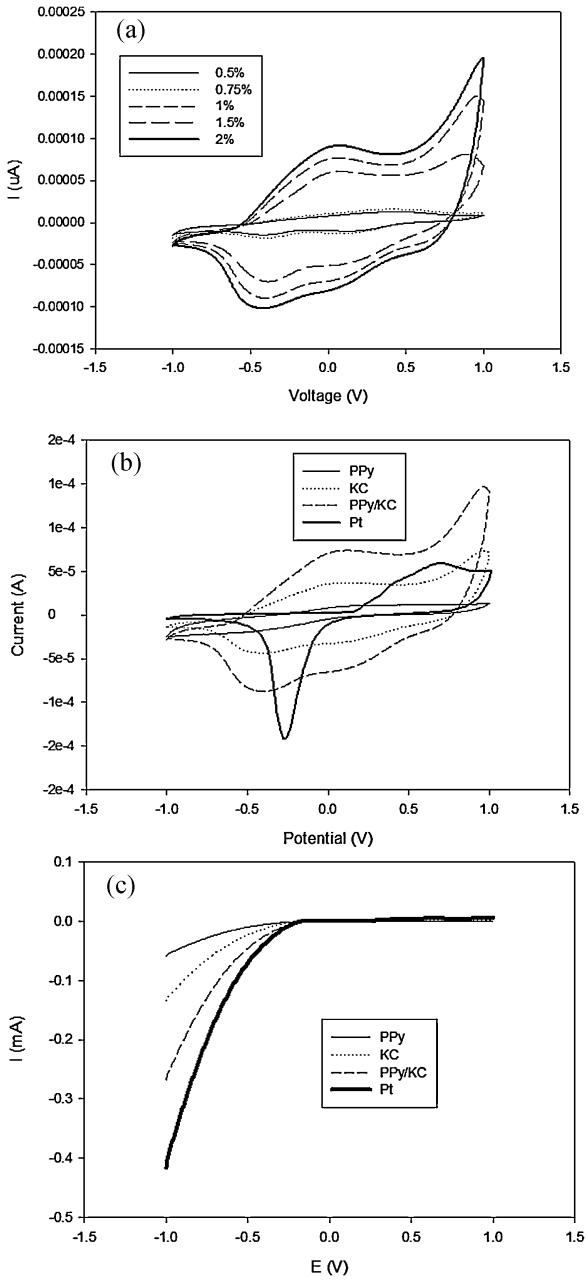

Fig. 6. (a) Effect of KC concentration on the growth of composite based on cyclic voltammetry. (b) The comparison of cyclic voltammetry at scan rate of 0.05 V/s PPy, KC, PPy/KC and Pt onto SPE in 0.01 M PBS solution, (c) LSV of the samples.

with a wide conductive region. Moreover, the background current of the PPy/KC was apparently larger than that of PPy and KC, which indicates that the PPy/KC-modified electrode has a larger effective surface area. The current of the PPy/KC composite was shown to be better than that of the naked PPy and KC.

The PPy capability was exhibited in the reverse scan by conducting an oxidation to the anodic potential (0.1 V, doped) and then

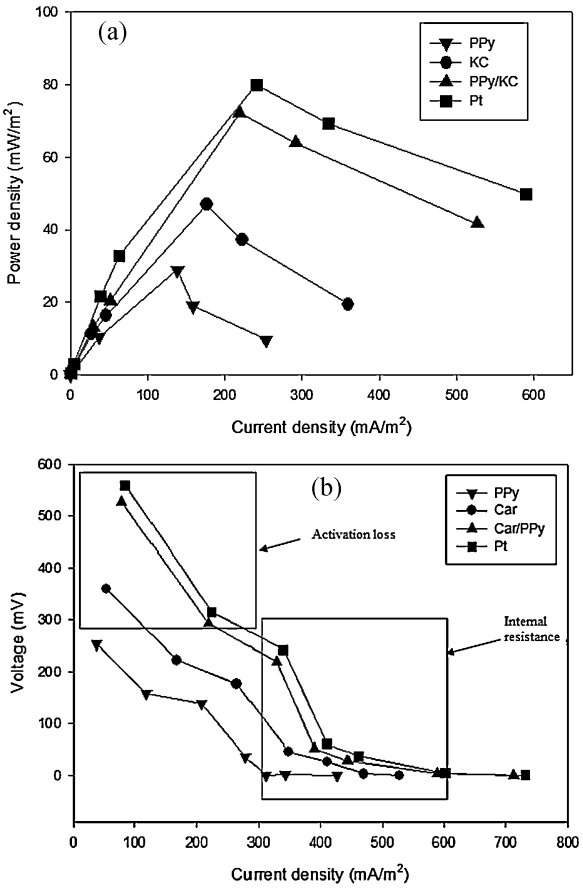

Fig. 7. (a) Power density graph of the MFCs (b) Polarization curve of the MFCs.

reduced by polarization at the cathodic potential (−0.6 V, undoped) (Otero, Arias-Pardilla, & Chermak, 2010) via the cyclic voltammetry method.

Growth of the polymer depends on the interaction of $-OSO_3^-$ (sulphate) group of the KC polyanion with the positive charge on the pyrrole monomer. The concentration of KC has a high impact on the electrical properties of the composite. It has been shown that by increasing the concentration of KC in the composite, the current increases. Maximum current was obtained from the composite that was prepared from 2% KC (Yuguchi, Thu Thuy, Urakawa, & Kajiwara, 2002). It was also shown in Fig. 6a. It is noteworthy, after optimum condition of KC has been achieved, at KC concentration above 2% the composite will be very stiff and cannot obtained homogenous solution thus, any further experiment was carried out at 2% KC concentration.

The LSV reduction of different catalysts and the resulting current is shown in Fig. 6b. It illustrates that PPy/KC has the highest ORR activity among the catalysts. The different LSV curve clarifies that the diffusion rate and ORR mechanisms of catalysts are different and so the overall electron transfer number must be different.

3.6. Power density and polarization curve

The power density generation of the MFCs with different cathode catalysts has been measured and the graph is shown in the Fig. 7a. As the figure shows, the MFC working with PPy has the lowest maximum power generation. It is about 28.8 mW/m^2 whereas KC produced 46.8 mW/m^2, which is 1.6 times more power than PPy. This can be due to some catalytic properties of KC which can do ORR better than PPy. The highest power generation was produced by the composite of PPy/KC. As can be seen in the figure, the maximum power generation of this catalyst is about 72.1 mW/m^2 at current density of 219.3 mA/m^2. Thus, the PPy/KC produced a higher power than KC and PPy. In comparison with Pt as the common and the most expensive cathode catalyst which produces 79.7 mW/m^2, the new bio-nano catalyst (PPy/KC) can produce 90.5% of that of Pt which can be a good achievement and is in a state of comparable current density.

Thus, the increase in the catalytic activity of the cathode by creating a composite cathode catalyst improved the ORR.

The polarization curve of the different MFCs is shown in Fig. 7b. The *I–V* curve slope, or the current versus the voltage, is the internal resistance of the MFC (Ieropoulos, Winfield, & Greenman, 2010). By calculating the *I–V* curve slope in the stable current density area, it can be seen that the internal resistance of the systems working with PPy and PPy/KC as cathode catalysts are quite same, around 560 Ω while the internal resistance of the system working with KC is about 610 Ω. The activation loss of the systems can also be observed in the polarization curve. Activation loss is the energy lost during the start of oxidation and at the reduction while other situations remain the same. In the system with higher power generation, higher activation loss is expected, but the graph shows that the activation loss of PPy/KC is quite the same with the two other systems. These results suggest that by applying a proper cathode catalyst even the activation loss is less than the amount which is expected (Ghasemi et al., 2013b,c).

Table 1
Summary of the data taken from the systems.

Catalyst	P_{max} (mW/m^2)	I_{max} at P_{max} (mA/m^2)	CE (%)	COD removal (%)	OCV at SS condition (mV)
PPy	28.8	138.6	6.7	74	497
KC	46.8	176.6	10.8	83	649
PPy/KC	72.1	219.3	16.7	98	784
Pt	79.7	233.5	18.4	85	812

3.7. COD removal and the coulombic efficiency

Table 1 reports all the information that have been taken from the MFC systems. This table also reports CE and COD removal of all of the systems. CE means the percentage of recovered electrons as current to the total coulombs in the substrate. As can be seen, the COD removals of the systems are 74%, 83 and 98% for the PPy, KC and PPy/KC composite, respectively, whilst their CEs are 6.7, 10.8 and 16.7%. It clarifies that the PPy is the weakest catalyst in this study as it cannot harvest electrons as much as the KC and PPy/KC composites. Definitely, PPy/KC as the best studied catalyst, does the ORR better than KC and PPy and converts more electrons to electricity. Also it keeps the pH of the system proper and does not disturb the microorganisms' metabolism and this is the reason for the high COD removal in the anode chamber (He, Minteer, & Angenent, 2005). It can be also seen that its CE can be compared to Pt as the CE of Pt is 18.4%. These results show the capability of PPy/KC to be an alternative for Pt.

4. Conclusions

This study demonstrated the use of a new nano-bio composite as an alternative for Pt as the cathode catalyst in a MFC. The novel spherical shape of PPy/KC showed an outstanding catalytic activity for ORR in the MFC. The PPy/KC could produce the power of about 91% of Pt. Although the power production of this cathode catalyst was lower than Pt, the power was higher than that of KC and PPy. It revealed the different structure of the composite in respect to the species that form that composite. On the other hand, it is the first nano-bio composite (PPy nano particle/KC bio polymer) that

has been used in a laboratory scale in the MFC system. These findings can provide a new window for identifying new composites for dealing with the problem of un-economical cathode catalysts (Pt) in MFCs.

Acknowledgment

The authors would like express their appreciation for the financial support given for this research by the Universiti Kebangsaan Malaysia (UKM) under research grants GGPM/2013/027, DIP-2012-11 and ERGS/1/2012/TK05/UKM/01/2.

References

Abdi, M. M., Mahmud, H. E., Kassim, A., Yunus, W. M. M., Talib, Z. A., & Haron, M. J. (2010). Synthesis and characterization of a new conducting polymer composite. *Polymer Science Series B*, *52*(11–12), 662–669.

Alves, V. D., Castelló, R., Ferreira, A. R., Costa, N., Fonseca, I. M., & Coelhoso, I. M. (2011). Barrier properties of carrageenan/pectin biodegradable composite films. *Procedia Food Science*, *1*, 240–245.

Andrenacci, N., Pieri, P., & Strinati, G. (2000). Size shrinking of composite bosons for increasing density in the BCS to Bose–Einstein crossover. *The European Physical Journal B—Condensed Matter and Complex Systems*, *13*(4), 637–642.

Apetrei, I. M., & Apetrei, C. (2013). Amperometric biosensor based on polypyrrole and tyrosinase for the detection of tyramine in food samples. *Sensors and Actuators B: Chemical*, *178*(0), 40–46.

Arora, K., Chaubey, A., Singhal, R., Singh, R. P., Pandey, M., Samanta, S., et al. (2006). Application of electrochemically prepared polypyrrole–polyvinyl sulphonate films to DNA biosensor. *Biosensors and Bioelectronics*, *21*(9), 1777–1783.

Ates, M., Karazehir, T., & Sarac, A. S. (2012). Conducting polymers and their applications. *Development*, *51*, 52.

Bakhshi, A., & Bhalla, G. (2004). Electrically conducting polymers: Materials of the twenty first century. *Journal of Scientific and Industrial Research*, *63*, 715–728.

Brezoi, D.-V. (2010). Polypyrrole films prepared by chemical oxidation of pyrrole in aqueous $FeCl_3$ solution. *Journal of Science and Arts*, *1*(12), 53–58.

Chen, F., Peng, J., Lei, D., Liu, J., & Zhao, G. (2013). Optimization of genistein solubilization by κ-carrageenan hydrogel using response surface methodology. *Food Science and Human Wellness*, *2*(3), 124–131.

Colin, C., & Petit, M. A. (2002). Electrochemical preparation and properties of films of polypyrrole/κ-carrageenan composites dependence on κ-carrageenan conformation. *Journal of the Electrochemical Society*, *149*(10), E394–E401.

Dharuman, V., Hahn, J. H., Jayakumar, K., & Teng, W. (2013). Electrochemically reduced graphene–gold nano particle composite on indium tin oxide for label free immuno sensing of estradiol. *Electrochimica Acta*, *114*, 590–597.

Fujishima, M., Takatori, H., Yamai, K., Nagao, Y., Kitagawa, H., & Uchida, K. (2008). Proton conductivity of biopolymer–platinum nanoparticle composite under high humidity. *Journal of Materials Science*, *43*(9), 3130–3134.

Ghasemi, M., Daud, W. R. W., Hassan, S. H. A., Oh, S.-E., Ismail, M., Rahimnejad, M., et al. (2013). Nano-structured carbon as electrode material in microbial fuel cells: A comprehensive review. *Journal of Alloys and Compounds*, *580*(0), 245–255.

Ghasemi, M., Daud, W. R. W., Rahimnejad, M., Rezayi, M., Fatemi, A., Jafari, Y., et al. (2013). Copper–phthalocyanine and nickel nanoparticles as novel cathode catalysts in microbial fuel cells. *International Journal of Hydrogen Energy*, *38*(22), 9533–9540.

Ghasemi, M., Ismail, M., Kamarudin, S. K., Saeedfar, K., Daud, W. R. W., Hassan, S. H. A., et al. (2013). Carbon nanotube as an alternative cathode support and catalyst for microbial fuel cells. *Applied Energy*, *102*(0), 1050–1056.

Ghasemi, M., Rahimnejad, M., Esmaeili, C., Daud, W. R. W., Masdar, M. S., Majlan, E. H., et al. (2013). Polysulfone composed of polyaniline nanoparticles as nanocomposite proton exchange membrane in microbial fuel cell. *American Journal of Biochemistry and Biotechnology*, *8*(4), 311.

Ghasemi, M., Shahgaldi, S., Ismail, M., Kim, B. H., Yaakob, Z., & Wan Daud, W. R. (2011). Activated carbon nanofibers as an alternative cathode catalyst to platinum in a two-chamber microbial fuel cell. *International Journal of Hydrogen Energy*, *36*(21), 13746–13752.

Ghasemi, M., Shahgaldi, S., Ismail, M., Yaakob, Z., & Daud, W. R. W. (2012). New generation of carbon nanocomposite proton exchange membranes in microbial fuel cell systems. *Chemical Engineering Journal*, *184*, 82–89.

He, Z., Minteer, S. D., & Angenent, L. T. (2005). Electricity generation from artificial wastewater using an upflow microbial fuel cell. *Environmental Science & Technology*, *39*(14), 5262–5267.

Ieropoulos, I., Winfield, J., & Greenman, J. (2010). Effects of flow-rate, inoculum and time on the internal resistance of microbial fuel cells. *Bioresource Technology*, *101*(10), 3520–3525.

Liu, B., Zhang, D., Wang, J., Chen, C., Yang, X., & Li, C. (2013). Multilayer magnetic composite particles with functional polymer brushes as stabilizers for gold nanocolloids and their recyclable catalysis. *The Journal of Physical Chemistry C*, *117*(12), 6363–6372.

Lupu, S., Lete, C., Balaure, P. C., Caval, D. I., Mihailciuc, C., Lakard, B., et al. (2013). Development of amperometric biosensors based on nanostructured tyrosinase–conducting polymer composite electrodes. *Sensors*, *13*(5), 6759–6774.

Martínez-Huitle, C. A., & Brillas, E. (2009). Decontamination of wastewaters containing synthetic organic dyes by electrochemical methods: A general review. *Applied Catalysis B: Environmental*, *87*(3), 105–145.

Nguyet, T. T. M., Chi, T. Q., Yen, Q. T. H., Toan, N. T., Trung, N. Q., & Hung, L. T. (2013). Preparation, characterisation and catalytic activity of gold nanoparticles supported on Co_3O_4. *International Journal of Nanotechnology*, *10*(3), 334–342.

Otero, T., Arias-Pardilla, J., & Chermak, E. (2010). Reactive polymer films: Polypyrrole oxidation kinetics in aqueous solution. *Synthetic Metals*, *160*(5), 425–431.

Rahimnejad, M., Ghasemi, M., Najafpour, G. D., Ismail, M., Mohammad, A. W., Ghoreyshi, A. A., et al. (2012). Synthesis, characterization and application studies of self-made Fe_3O_4/PES nanocomposite membranes in microbial fuel cell. *Electrochimica Acta*, *85*(0), 700–706.

Reddy, K. R., Jeong, H. M., Lee, Y., & Raghu, A. V. (2010). Synthesis of MWCNTs-core/thiophene polymer-sheath composite nanocables by a cationic surfactant-assisted chemical oxidative polymerization and their structural properties. *Journal of Polymer Science Part A: Polymer Chemistry*, *48*(7), 1477–1484.

Reddy, K. R., Lee, K.-P., & Gopalan, A. I. (2007). Self-assembly directed synthesis of poly(*ortho*-toluidine)-metal (gold and palladium) composite nanospheres. *Journal of Nanoscience and Nanotechnology*, *7*(9), 3117–3125.

Reddy, K. R., Lee, K. P., & Iyengar, A. G. (2007). Synthesis and characterization of novel conducting composites of Fe_3O_4 nanoparticles and sulfonated polyanilines. *Journal of Applied Polymer Science*, *104*(6), 4127–4134.

Reddy, K. R., Sin, B. C., Ryu, K. S., Kim, J.-C., Chung, H., & Lee, Y. (2009). Conducting polymer functionalized multi-walled carbon nanotubes with noble metal nanoparticles: Synthesis, morphological characteristics and electrical properties. *Synthetic Metals*, *159*(7), 595–603.

Roberts, J. N., Buck, C. B., Thompson, C. D., Kines, R., Bernardo, M., Choyke, P. L., et al. (2007). Genital transmission of HPV in a mouse model is potentiated by nonoxynol-9 and inhibited by carrageenan. *Nature Medicine*, *13*(7), 857–861.

Sadeghi, M. (2012). Synthesis of a biocopolymer carrageenan-*g*-poly(AAm-*co*-IA)/montmorilonite superabsorbent hydrogel composite. *Brazilian Journal of Chemical Engineering*, *29*(2), 295–305.

Safarnavadeh, V., Zare, K., & Fakhari, A. R. (2013). Capability of parasulfonato calixarene, as an anion dopant, and organic solvents in enhancing the sensitivity and loading of glucose oxidase (GOx) on polypyrrole film in a biosensor: A comparative study. *Biosensors and Bioelectronics*, *49*(0), 159–163.

Saville, P. (2005). Polypyrrole, formation and use. In *DTIC document*. DTIC.

Shinde, S. S., Gund, G. S., Dubal, D. P., Jambure, S. B., & Lokhande, C. D. (2013). Morphological modulation of polypyrrole thin films through oxidizing agents and their concurrent effect on supercapacitor performance. *Electrochimica Acta*.

Wang, L.-X., Li, X.-G., & Yang, Y.-L. (2001). Preparation, properties and applications of polypyrroles. *Reactive and Functional Polymers*, *47*(2), 125–139.

Yalçınkaya, S., Demetgül, C., Timur, M., & Çolak, N. (2010). Electrochemical synthesis and characterization of polypyrrole/chitosan composite on platinum electrode: Its electrochemical and thermal behaviors. *Carbohydrate Polymers*, *79*(4), 908–913.

Yuguchi, Y., Thu Thuy, T. T., Urakawa, H., & Kajiwara, K. (2002). Structural characteristics of carrageenan gels: Temperature and concentration dependence. *Food Hydrocolloids*, *16*(6), 515–522.

Zhang, H., Xu, M., Cui, R., Guo, X., Yang, S., Liao, L., Jia, Q., Chen, Y., Dong, J., & Sun, B. (2013). Enhanced performance of inverted organic photovoltaic cells using CNTs–TiO_X nanocomposites as electron injection layer. *Nanotechnology*, *24*(35), 355401.